Earthquakes and Structures, *Vol. 9, No. 1 (2015) 73-91*
DOI: http://dx.doi.org/10.12989/eas.2015.9.1.073

Seismic effectiveness of tuned mass dampers in a life-cycle cost perspective

Emiliano Matta*

Department of Structural, Geotechnical and Building Engineering, Politecnico di Torino, C.so Duca degli Abruzzi 24, Turin, Italy

(Received September 6, 2013, Revised February 21, 2015, Accepted February 23, 2015)

Abstract. The effectiveness of tuned mass dampers (TMDs) in reducing the seismic response of civil structures is still a debated issue. The few studies regarding TMDs on inelastic structures indicate that they would perform well under moderate earthquake loading, when the structure remains linear or weakly nonlinear, while tending to fail under severe ground shaking, when the structure experiences strong nonlinearities. TMD seismic efficiency should be therefore rationally assessed by considering to which extent moderate and severe earthquakes respectively contribute to the expected cost of damages and losses over the lifespan of the structure. In this paper, a method for evaluating, in a life-cycle cost (LCC) perspective, the seismic effectiveness of TMDs on inelastic building structures is presented and exemplified on the SAC LA 9-storey steel moment-resisting frame benchmark building. Results show that the LCC concept may provide an appropriate alternative to traditional performance criteria for the evaluation of the effectiveness of TMDs and that TMD installation on typical existing middle-rise buildings in high seismic hazard regions may significantly reduce building lifetime cost despite the poor control performance observed under the most severe seismic events.

Keywords: structural control; tuned mass dampers (TMD); existing structures; nonlinear dynamic analysis; life-cycle cost analysis; cost-effectiveness

1. Introduction

In recent years, several vibro-protecting strategies have been developed for improving serviceability and safety of civil structures against natural and manmade hazards. Passive control systems have been installed in a number of full-scale buildings throughout the world (Soong and Dargush 1997). Among them, the passive tuned mass damper (TMD) has been deeply studied and widely applied on both new and existing structures because of its simplicity, efficiency and low maintenance cost. In its basic configuration, a TMD is a single-degree-of-freedom (SDOF) appendage of the primary structure. By properly tuning its natural frequency to that of the selected structural target mode, a significant part of the vibratory energy of that mode is transferred to the appendage and dissipated through its damping (Warburton 1982). Commonly used for controlling the response of flexible structures to wind, water waves and traffic loading (Homma *et al*. 2009),

*Corresponding author, Research Scholar, Ph.D., E-mail: emiliano.matta@polito.it

http://www.techno-press.org/journals/eas&subpage=7 ISSN: 2092-7614 (Print), 2092-7622 (Online)

TMDs are more rarely employed for the seismic protection of buildings, their effectiveness in earthquake mitigation still being fairly controversial.

Numerous available results show that TMDs can satisfactorily reduce the seismic response of structures as long as these remain linear (e.g., Villaverde and Koyama 1993, Sadek *et al.* 1997). Their effectiveness is larger for long-duration narrow-band ground motions, but has recently been proven acceptable even against impulsive earthquakes provided that sufficiently large mass ratios and proper design techniques are adopted (Hoang *et al.* 2008, Matta 2011, 2013).

Fewer researchers have considered TMDs on inelastic structures under earthquake loading. Although a certain controversy still exists on this subject, TMDs efficiency is generally admitted to substantially decrease when the primary structure experiences a nonlinear response, especially in terms of peak response reduction. Kaynia *et al.* (1981) assessed the seismic effectiveness of TMDs on elastic-perfectly plastic SDOF systems under historical seismic records, finding a small reduction in the cumulative yielding ductility and an insignificant reduction in the ductility ratio. Sladek and Klingner (1983) studied the effect of a light TMD on a 25-storey building experiencing stiffness degradation under the 1940 El Centro record, concluding that peak displacement was almost unaffected by the TMD, and yielding at the base of the core walls could not be eliminated. Chowdhury *et al.* (1985) evaluated the same inelastic building under various earthquake records, reporting that the controlled peak response ranged from 0.74 to 1.05 times the uncontrolled response depending on the values taken by the TMD mass ratio (varying from 5% to 18%) and damping ratio (ranging from 4% to 19%). Examining the behaviour of an inelastic SDOF structure-TMD system under the 1985 Mexico City excitation, Bernal (1996) found that the peak displacement reduction decreased with increasing inelastic excursions. Studying TMDs on nonlinear structures, Ruiz and Esteva (1997) concluded that their effectiveness in reducing the peak response becomes small as non-linearity increases. Soto-Brito and Ruiz (1999) studied the effect of ground motion characteristics on the effectiveness of TMDs in reducing the maximum displacement of a 22-storey nonlinear structure subject to moderate- and high-intensity earthquakes; the TMD proved successful for moderate but not for severe earthquakes. Considering the peak response reduction an insufficient criterion for assessing the seismic effectiveness of TMDs on inelastic structures, Lukkunaprasit and Wanitkorkul (2001) and Pinkaew *et al.* (2003) adopted the accumulated hysteretic energy ratio as the performance index to measure the low-cycle fatigue damage induced by ground motion; they showed that, although a TMD cannot effectively reduce the peak displacement of the controlled structure after yielding, it can significantly reduce fatigue damage under moderate earthquakes. The same energy perspective was adopted by Wong (2008), who showed that TMDs enhance the ability of inelastic structures to withstand strong earthquakes by storing large amounts of energy at the critical moments and subsequently releasing them in the form of damping energy. An approach based on seismic fragility curves was adopted by Wong and Harris (2012) to investigate the effectiveness of a TMD on an inelastic 6-storey steel moment-resisting frame (MRF); results showed that a TMD can enhance the structure’s ability to dissipate energy at low levels of earthquake shaking but is less effective during strong earthquakes. Zhang and Balendra (2013) explored the performance of TMDs on weakly-nonlinear structures in areas subjected to narrow-band long-distance earthquakes; applying their proposed optimization criterion to a TMD having 2% mass ratio and installed on a weakly-nonlinear SDO-structure under a narrow-band long-duration record, they obtained a 19% displacement reduction instead of the 16% provided by traditional design methods.

The current state of the art thus seems to indicate that TMDs can keep effective under moderate earthquake loading, when the structure remains linear or weakly nonlinear, while tending to fail under severe ground shaking, when the structural response becomes strongly nonlinear. As a consequence, a fair and thorough assessment of TMDs seismic efficiency should necessarily be founded on determining, based on a probabilistic seismic hazard description, to which extent moderate and severe earthquakes respectively contribute to the expected damage cost over the lifespan of the structure, i.e., on establishing how TMDs actually impact on the structure life-cycle cost (LCC).

LCC assessment is a decision-support tool increasingly used in several fields of engineering for evaluating the efficiency of systems. In earthquake engineering, it is employed as a structural performance criterion accounting for the expected cost of future seismic damages and losses, defined by applying a cost factor to the failure probability of the structure. By applying the LCC concept, instead of merely looking at an asset in terms of costs to design and build (initial cost), investors and managers can broaden their perspective including all operation, maintenance, repair, replacement and disposal costs over a period of time (lifetime cost). The sum of the initial and the lifetime costs determines the total LCC of the building, whose minimization should be the primary goal of any optimal design action, either in constructing a new structure or in retrofitting an existing one. LCC assessment of structures in seismic areas has been the subject of several studies in the last decade (e.g., Beck *et al.* 2003, Sanchez-Silva and Rackwitz 2004, Goulet *et al.* 2007, Kappos and Dimitrakopoulos 2008), including some recent works focusing on passive (Taflanidis and Beck 2009) and semi-active (Hahm *et al.* 2013) control strategies. To the best of the author's knowledge, no application of LCC analysis to structures controlled by means of TMDs has ever been reported in the literature, nor any other study specifically focused on the economic advantages of TMDs in earthquake mitigation of building structures.

In the present paper, a method for evaluating, in a LCC perspective, the seismic effectiveness of TMDs on inelastic building structures is presented and exemplified on the simulated case study of a seismic TMD-based retrofit of the 9-storey benchmark structure proposed within the SAC Phase II Steel Project (Gupta and Krawinkler 1999) as representative of typical middle-size steel MRF office buildings designed for the Los Angeles area.

2. Methodology

Various methods have been developed to estimate lifetime cost in earthquake engineering (Taflanidis and Beck 2009). Among these methods, the approach developed by Wen and Kang (2001) and subsequently improved by Lagaros and co-authors (e.g., Lagaros *et al.* 2006, Fragiadakis and Lagaros 2011, Mitropoulou *et al.* 2011) appears particularly appealing for its simplicity. The approach makes damage and consequently lifetime cost depend, for any assigned structural type (in the present example: steel MRF buildings), on one or more seismic demand parameters evaluated at multiple hazard levels through static or dynamic nonlinear analyses. Since the structure-TMD interaction phenomenon can only be described in terms of time-history response, the variant relying on nonlinear dynamic analyses is implemented here.

2.1 Seismic response evaluation

In earthquake engineering, LCC assessment requires the calculation of cost components that are related to the performance of the structure in multiple seismic hazard levels. Incremental static and dynamic analyses are two available procedures for estimating the seismic response of a structural system which can be incorporated into the LCC assessment methodology (Vamvatsikos and Cornell 2002). In the present study the so-called multiple-stripe dynamic analysis (MSDA) is adopted, one of the most applied multiple-hazard methods implementing nonlinear dynamic analysis. In MSDA, many groups of nonlinear dynamic analyses (stripes) are performed at increasing intensity levels, each level corresponding to a predetermined exceedance probability in a given period. The suite of ground motion records used for performing each stripe analysis should be representative of the seismic threat at the corresponding intensity, according to the hazard curve of the area of interest. The main objective of MSDA is to express the relation existing between the seismic intensity level, described by a parameter (or a vector of parameters) known as the intensity measure (IM), and the corresponding structural response, described by an engineering demand parameter (EDP), sometimes referred to as the damage index (DI). A probabilistic seismic hazard analysis is usually performed to characterize IMs for different hazard levels, taking into account all important sources of modelling uncertainty for the ground motions. Typically only a small number of hazard levels are considered. For each of these levels, ground motion records consistent with the corresponding IMs are selected from some strong-motion database by performing a seismic hazard disaggregation. These records are taken to represent samples of possible future ground motions for each hazard level and are used in MSDA to extract samples of the structural response and to eventually computed the EDP required for cost estimation. Due to the complexity and the computational effort required by 3D structural models, simplified 2D simulations are frequently used in the analysis. This is justified for plan-symmetric buildings and particularly in the case of steel framed buildings composed by 2D MRF structures.

Selecting IM and EDP is one of the fundamental steps in MSDA. The IM is typically a monotonically scalable ground motion intensity measure like, among others, the peak ground acceleration, the peak ground velocity or the 5% damped spectral acceleration at the structure's first-mode period. On the other hand, EDPs can be classified in four main categories (Ghobarah *et al.* 1999): EDPs based on maximum deformation; EDPs based on cumulative damage; EDPs accounting for maximum deformation and cumulative damage; and global EDPs. There is wide consensus that for MRF structures the storey drift demand, expressed in terms of the inter-storey drift ratio θ, is the best representative of the first category of EDPs at the storey level (Gupta and Krawinkler 1999). An established relation exists between θ and performance-oriented descriptions, such as immediate occupancy, life safety and collapse prevention (FEMA-273 1997). Definite relations, required for LCC assessment, are also available between θ and damage state, for both reinforced concrete buildings (Ghobarah 2004) and steel frame structures (Wen and Kang 2001).

Table 1 Damage states in terms of drift ratio (Wen and Kang 2001)

Damage state	Drift ratio θ (%)
1-None	$0.0 \le \theta < 0.2$
2-Slight	$0.2 \le \theta < 0.5$
3-Light	$0.5 \le \theta < 0.7$
4-Moderate	$0.7 \le \theta < 1.5$
5-Heavy	$1.5 \le \theta < 2.5$
6-Major	$2.5 \le \theta < 5.0$
7-Destroyed	$5.0 \le \theta$

The use of the inter-storey drift ratio is furthermore recommended by FEMA-350 (2000) as the most suitable performance criterion for frame structures.

In the illustrative example reported in Section 3, MSDA will be implemented using seven hazard levels, each described by a set of ten 2-component earthquake records selected to be compatible with the corresponding earthquake response spectrum at the site. The peak inter-storey drift ratio θ will be chosen as the EDP and the relation between damage state and inter-storey drift ratio will be the one proposed by Wen and Kang (2001) for steel MRF structures, reproduced in Table 1. In order to extract the EDP for each hazard level, the 2D FE structural model will be separately evaluated under each component of any record so as to obtain the component-EDP; then the larger of the two component-EDPs of each record will be taken as the record-EDP; and finally the mean among all record-EDPs of each set of records will give the set-EDP, eventually used for cost assessment.

2.2 Cost evaluation

According to Wen and Kang (2001) and Lagaros *et al.* (2006), the expected total cost C_{TOT} of a structure (either uncontrolled or controlled), over a time period t which may be the design life of a new structure or the remaining life of a retrofitted structure, can be expressed as a function of t as follows

$$C_{TOT}(t) = C_{IN} + C_{DS}(t) \tag{1}$$

where C_{IN} is the initial cost of a new or retrofitted structure and C_{DS} is the additional cost over the lifetime of the structure, defined as the present value of future damage states' costs. C_{IN} refers to the material and labour costs required for the construction of a new building or the retrofitting of an existing one, including structural and non-structural components. C_{DS} refers to the potential damage cost from earthquakes that may occur during the life of the structure, i.e., the seismic lifetime cost. It accounts for the cost of structural and non-structural repair, the cost of loss of contents, the cost of injury recovery or human fatality and other direct or indirect economic losses (e.g., rental and income costs), after an earthquake. The quantification of the losses in economic terms depends on several socio-economic parameters. The most difficult cost to quantify is the cost corresponding to the loss of human lives. There are a number of approaches for its estimation, ranging from purely economic reasoning to more sensitive ones that consider irreplaceable the loss of a human being. Therefore, estimating the cost of exceeding the collapse damage state will vary considerably according to which approach is adopted.

Considering N possible damage states (N=7 in the present case study, see again Table 1), the cost related to the i-th damage state can be formulated as follows (Mitropoulou *et al.* 2011)

$$C_{DS}^{i} = C_{dam}^{i} + C_{con}^{i} + C_{ren}^{i} + C_{inc}^{i} + C_{inj}^{i} + C_{fat}^{i} \tag{2}$$

where C_{dam}^{i} is the damage repair cost, C_{con}^{i} is the loss of contents cost, C_{ren}^{i} is the rental loss cost, C_{inc}^{i} is the income loss cost, C_{inj}^{i} is the injury cost and C_{fat}^{i} is the human fatality cost. Details about the evaluation of each damage state cost can be found in Table 2 (Wen and Kang 2001), where the basic costs (in the third column) represent the first component of the calculation formulas (in the second column). The damage state parameters, i.e., the mean damage index, the loss of function index, the down time index, the expected minor injury rate, the expected serious injury rate and the expected death rate, are derived by Mitropoulou *et al.* (2011) and reported in Table 3.

Table 2 Damage state cost calculation formulas (Wen and Kang 2001)

Cost category	Calculation formula	Basic cost
Damage repair	Replacement cost×floor area×mean damage index	1500 €/m^2
Loss of content	Unit content cost×floor area×mean damage index	500 €/m^2
Rental	Rental rate×gross leasable area $^{(ii)}$×disruption period $^{(iii)}$×loss of function index	10 €/month/m^2
Income	Income rate×gross leasable area $^{(ii)}$×disruption period $^{(iii)}$×down time index	2000 €/year/m^2
Minor injury	Minor injury cost per person×floor area×occupancy rate $^{(i)}$×expected minor injury rate	2000 €/person
Serious injury	Serious injury cost per person×floor area×occupancy rate $^{(i)}$×expected serious injury rate	$2 \cdot 10^4$ €/person
Human fatality	Death cost per person×floor area×occupancy rate $^{(i)}$×expected death rate	$2.8 \cdot 10^6$ €/person

$^{(i)}$ Occupancy rate: 2 persons/100 m^2
$^{(ii)}$ Gross leasable area: 90% of the total floor area
$^{(iii)}$ Disruption period: 6 months

Table 3 Damage state parameters for cost evaluation (Mitropoulou *et al.* 2011)

Damage state	Mean damage index (%)	Loss of function index (%)	Down time index (%)	Expected minor injury rate	Expected serious injury rate	Expected death rate
1-None	0	0	0	0	0	0
2-Slight	0.5	0.9	0.9	$3.0 \cdot 10^{-5}$	$4.0 \cdot 10^{-6}$	$1.0 \cdot 10^{-6}$
3-Light	5	3.33	3.33	$3.0 \cdot 10^{-4}$	$4.0 \cdot 10^{-5}$	$1.0 \cdot 10^{-5}$
4-Moderate	20	12.4	12.4	$3.0 \cdot 10^{-3}$	$4.0 \cdot 10^{-4}$	$1.0 \cdot 10^{-4}$
5-Heavy	45	34.8	34.8	$3.0 \cdot 10^{-2}$	$4.0 \cdot 10^{-3}$	$1.0 \cdot 10^{-3}$
6-Major	80	65.4	65.4	$3.0 \cdot 10^{-1}$	$4.0 \cdot 10^{-2}$	$1.0 \cdot 10^{-2}$
7-Destroyed	100	100	100	$4.0 \cdot 10^{-1}$	$4.0 \cdot 10^{-1}$	$2.0 \cdot 10^{-1}$

Based on a Poisson process model of earthquake occurrences and the assumption that damaged buildings are fully and quickly restored to their original intact conditions after each significant seismic attack, the damage state cost in Eq. (1) can be computed using the following formula (Wen and Kang 2001)

$$C_{DS}(t) = \nu \left(\frac{1-e^{-\lambda t}}{\lambda} \right) \sum_{i=1}^{N} C_{DS}^{i} P_{o}^{i} \tag{3}$$

where P_o^i is the probability of occurrence of the i-th damage state given the occurrence of a significant earthquake; ν is the mean frequency of occurrence of significant earthquakes, modelled by a Poisson process; and λ is the momentary discount rate, introduced to actualize future costs to their current value and herein assumed equal to 4%/year. The ratio in parenthesis, which tends to t for λ tending to 0, represents the actualized time period $t_a = \rho_a t$, where $\rho_a = (1-e^{-\lambda t})/\lambda t$ is the actualization cost ratio (or present worth factor), so Eq. (3) can also be rewritten as

$$C_{DS}(t) = (\nu t)\sum_{i=1}^{N}(\rho_a C_{DS}^i)P_o^i \tag{4}$$

where νt is the expected number of significant earthquakes in t and $\rho_a C_{DS}^i$ is the actualized cost of the i-th damage state, or even more conveniently as

$$C_{DS}(t) = t_a \sum_{i=1}^{N} C_{DS}^i \phi_o^i \tag{5}$$

where $\phi_o^i = \nu P_o^i$ is the mean frequency of occurrence of the i-th damage state. Following Wen and Kang (2001), the i-th damage state is identified by the drift ratio limits listed in Table 1. When one of those limits is exceeded, the corresponding damage state is reached. In other words, in order for the i-th damage state to occur, the i-th limit θ_i must have been exceeded while the (i+1)-th limit θ_{i+1} must have not. As a result, the occurrence frequency ϕ_o^i in Eq. (5) can be computed as

$$\phi_o^i = \phi_e^i - \phi_e^{i+1} \tag{6}$$

where ϕ_e^i, representing the mean frequency of exceedance of θ_i, can be expressed by a relation of the form

$$\phi_e^i = f(\theta_i) \tag{7}$$

Eq. (7) is deduced by fitting a properly shaped function f to M known $\phi_e^j - \theta_j$ pairs, each corresponding to a preselected hazard level (i.e., a given set of records) characterized by a known probability of exceedance $P_{e/\tau}^j$ in the time period τ. For each hazard level, θ_j is the set-EDP computed through nonlinear dynamic analyses, while ϕ_e^j is the mean frequency of exceedance of θ_j and can be derived, according to Poisson's law, as

$$\phi_e^j = -\frac{1}{\tau}\ln(1 - P_{e/\tau}^j) \tag{8}$$

In previous works by, e.g., Lagaros *et al.* (2006) and Mitropoulou *et al.* (2011), the relation expressed by Eq. (7) is obtained by a least-square fitting of the M pairs through a hyperbolic function of the form

$$f(\theta) = \alpha\theta^{-\beta} \tag{9}$$

Depending on two fitting parameters, α and β, Eq. (9) ensures an exact fitting for M=2 but generally causes some error for M>2. For the case study under analysis, the error was observed to be unacceptably large already for M as small as 3 or 4 (implying biased cost estimates) and Eq. (9) was concluded to be inadequate for fitting. Also, taking M=3, as in some previous studies, proved here insufficient to sample the entire domain of possible pairs. Various alternative functional forms for f were then explored, which might work properly for larger values of M (e.g., M=7 as in the present cast study). A good compromise between simplicity and accuracy was obtained adopting the following expression

$$f(\theta) = \begin{cases} \alpha_1\theta^{-\beta_1} & for\,\theta < \theta_2 \\ \gamma(\alpha_j\theta^{-\beta_j}) + (1-\gamma)(a_j\theta + b_j) & for\,\theta_j \le \theta < \theta_{j+1},\ j = 2,\ldots,M-2 \\ \alpha_{M-1}\theta^{-\beta_{M-1}} & for\,\theta \ge \theta_{M\text{-}1} \end{cases} \tag{10}$$

where α_j and β_j are analytically determined so that the hyperbolic function $\alpha_j \theta^{-\beta_j}$ exactly interpolates pairs j and j+1, a_j and b_j are analytically determined so that the linear function $a_j\theta + b_j$ exactly interpolates pairs j and j+1, and the weight γ is numerically determined so that the sum of the changes of slope of $f(\theta)$ at every θ_j, expressed by $\sum_{j=2}^{M-1} \left| f'_+(\theta_j) - f'_-(\theta_j) \right|$, shall be minimum. In the range [θ_2, θ_{M-1}], Eq. (10) provides the weighed sum of the hyperbolic interpolation and the linear interpolation of the M–2 internal pairs, performed independently between any two consecutive pairs. The merge of these two types of curves allows smoothing the angular points which would occur at the internal pairs if either type was used alone. Outside that range, Eq. (10) provides the hyperbolic exact fitting of the two outermost couples (respectively left and right) of $\phi_e^j - \theta_j$ pairs. As a result, Eq. (10) ensures a function passing through all the available M pairs. The minimization required to identify the optimal weight γ can be easily performed using any available numerical technique, including a simple trial & error search. An example of curves describing Eq. (10) will be discussed later (Fig. 5).

Unlike in previous works (e.g., Wen and Kang 2001, or Lagaros *et al.* 2006) in which the drift ratio was taken as the largest over the entire building height (maximum drift ratio), here damage and costs at any given storey are assumed to only depend on the drift ratio occurred at that particular storey, and the global building cost is finally obtained as the sum of all storey-level costs. The only exception is represented by costs related to the collapse damage state ("7-Destroyed"), which are still assumed to be governed, for all the storey levels, by the maximum drift ratio along the height of the building, as if the collapse of any one storey implied the collapse of the entire structure.

3. Example

The seismic cost-effectiveness of installing a TMD on an existing standard medium-rise office building is assessed by comparing its lifetime cost in, respectively, the absence and the presence of the control device atop. The building is a standard perimeter steel MRF structure located in Los Angeles (California). Because of its in-plan symmetry, structural analysis and cost evaluation will be performed using a planar (2D) model along the N-S direction only.

3.1 The structural system with and without TMD

3.1.1 The benchmark building

The case study is the 9-storey steel MRF building structure designed for Los Angeles by Brandow & Johnston Associates within the SAC Phase II Steel Project (Gupta and Krawinkler 1999), and later turned into one of the three benchmark control problems for seismically excited nonlinear buildings described in Ohtori *et al.* (2001). The structure is designed according to UBC 1994, following all code requirements for gravity, wind and seismic design. Although not actually constructed, it can be considered as representative of typical medium-rise steel MRF office building structures in LA designed according to pre-Northridge design practice.

The benchmark structure is 45.73 m by 45.73 m in plan and 37.19 m in elevation. The bays are 9.15 m on centre, in both directions, with five bays each in the North-South (N-S) and East-West (E-W) directions. The lateral load-resisting system is made of perimeter steel MRFs with simple

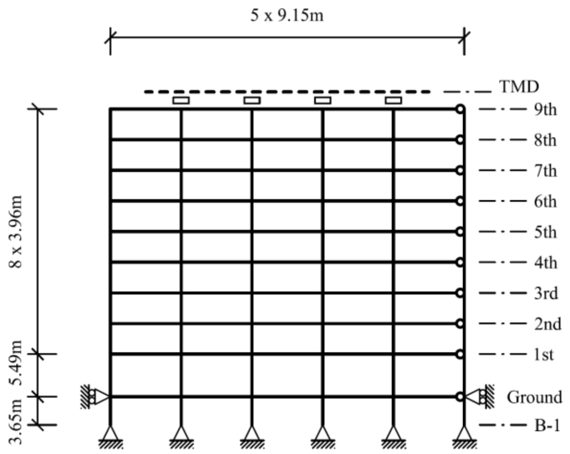

(a) Elevation

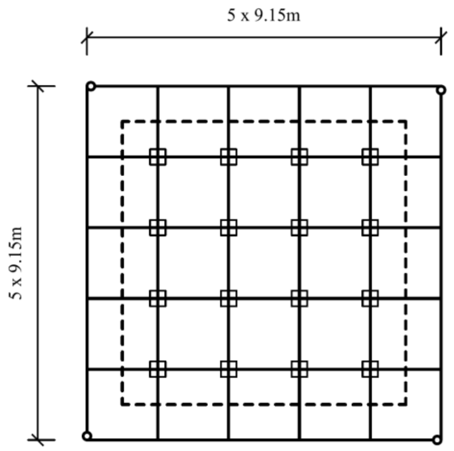

(b) Plan

Fig. 1 Schematics of the 9-storey building

framing on one of the exterior bays so as to avoid bi-axial bending in the corner column. The interior bays of the structure contain simple framing with composite floors. The building comprises one basement level, one ground level and nine above-ground levels, the ninth of which is the roof. Typical floor-to-floor heights are 3.96 m, but they are 3.65 m and 5.49 m for, respectively, the basement and the first floor. The column bases are modelled as pinned and secured to the ground at the B-1 level. Concrete foundation walls and surrounding soil are assumed to restrain the structure at the ground level from horizontal displacement. Dimensions and materials of columns and beams are detailed in Gupta and Krawinkler (1999). The inertial effects of each level are assumed to be carried evenly by the floor diaphragm to each perimeter MRF, hence each frame resists one half of the seismic mass associated with the entire structure. The seismic mass for the ground level is $9.65\cdot10^5$ kg, for the first level is $1.01\cdot10^6$ kg, for the second through eighth levels is $9.89\cdot10^5$ kg and for the ninth level is $1.07\cdot10^6$ kg. The N-S MRF is sketched in Fig. 1.

3.1.2 The uncontrolled structural model

The uncontrolled structural model is the 2D nonlinear FE representation of the two N-S MRFs of the benchmark building. The model is like the one implemented by Ohtori *et al.* (2001) in a set of MATLAB files available on the web (http://www.nd.edu/~quake/), except that in the present version it has been modified so as to account for second order (P-delta) effects and to allow incorporation of the TMD into the model.

The model represents a ductile steel MRF structure with no strength and stiffness degradation in the element characteristics and no connection weld fractures. A concentrated plasticity model is assumed, with members remaining elastic and yielding occurring only at their ends, where point plastic hinges are schematized by a bilinear moment-rotation relationship with 3% strain-hardening. Inertial loads are uniformly distributed at the nodes of the respective level assuming a lumped mass formulation. The damping matrix is determined based on an assumption of Rayleigh damping, enforcing a 2% damping ratio onto the first two modes.

As long as the structure responds in the linear elastic range, the first three natural frequencies

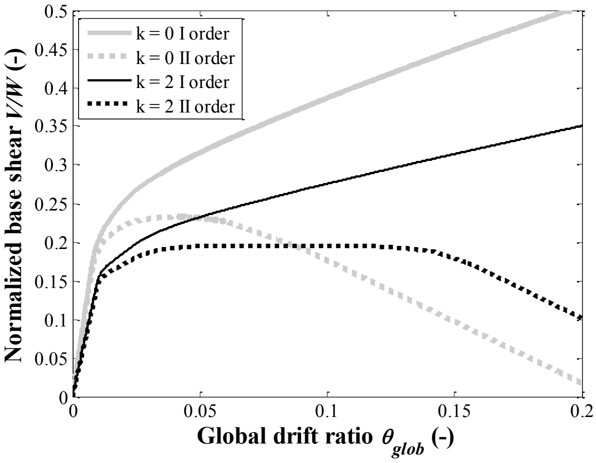

Fig. 2 Global pushover curves for the uncontrolled structural model, with or without II order effects

are 0.443 Hz, 1.18 Hz and 2.05 Hz for the model evaluated excluding second order effects, and 0.432 Hz, 1.15 Hz and 2.01 Hz for the model evaluated including second order effects. The pushover curves obtained for the uncontrolled structural model using either a uniform (k=0) or a quadratic (k=2) vertical pattern of horizontal accelerations are plotted in Fig. 2, with the global building drift ratio (defined as the displacement of the top storey divided by the building height) in the horizontal axis and the normalized base shear force in the vertical axis. The curves are consistent with those obtained by other authors (Gupta and Krawinkler 1999).

3.1.3 The controlled structural model

The controlled structural model is obtained by attaching to the top storey of the uncontrolled model a linear SDOF model of a TMD, characterized by a mass m_t, a circular frequency ω_t and a damping ratio ζ_t. The mass m_t is fixed by the designer as a given percentage of the total structural mass m_s through assigning the mass ratio $\mu=m_t/m_s$, whereas ω_t and ζ_t are chosen so as to achieve the optimum tuning of the absorber to the fundamental mode of the building. More precisely, denoting by ω_s and ζ_s respectively the circular frequency and damping ratio of the target mode, by $m_{s,eff}$ its effective modal mass, defined according to Warburton (1982) as the target modal mass divided by the squared amplitude of the mass-normalized target modeshape at the TMD position, and finally denoting by $\mu_{eff}=m_t/m_{s,eff}$ and $r=\omega_t/\omega_s$ respectively the effective mass ratio and the frequency ratio of the TMD, any design methodology will basically consist in: (i) arbitrarily fixing μ_{eff} based on cost-benefit considerations, and (ii) accordingly finding r and ζ_t which make the control be optimal with respect to some desired objective. Depending on the chosen objective, various analytical or numerical optimization criteria are available. The most widespread criteria aim at minimizing a given norm of some input-output transfer functions (TF) of the controlled system. Depending on the chosen norm, such criteria can be mainly distinguished into the H_2-norm design (Hoang *et al.* 2008) and the H_∞-norm design (Sladek and Klingner 1983, Pinkaew *et al.* 2003, Matta *et al.* 2009).

In the present study, the TF from the ground acceleration to the maximum inter-storey drift ratio, denoted as $T_{\theta u}$, is adopted, and the $H_\infty^{\,f}$ approach proposed in Matta (2011) is applied, which consists in the numerical minimization of the H_∞-norm of $T_{\theta u}$ multiplied by a Kanai-Tajimi filter

Table 4 Design control parameters for two possible values of TMD mass ratio

Mass ratio μ	Effective mass ratio μ_{eff}	Structural circular frequency ω_s	Frequency ratio r	Damping ratio ζ_t
5%	11.2%	2.71 rad/s	87.7%	19.2%
10%	22.5%	2.70 rad/s	78.1%	26.7%

Table 5 The M=7 multiple hazard levels considered in the present study

Set # j	1	2	3	4	5	6	7
$P^j_{e/\tau}$ (%)	50	50	50	50	50	10	2
τ (years)	2	5	10	30	50	50	50
ϕ^j_e (n/year)	$3.466 \cdot 10^{-1}$	$1.386 \cdot 10^{-1}$	$6.931 \cdot 10^{-2}$	$2.310 \cdot 10^{-2}$	$1.386 \cdot 10^{-2}$	$2.107 \cdot 10^{-3}$	$4.041 \cdot 10^{-4}$

whose circular frequency equals the structural frequency and whose damping ratio is set to 0.3. The linearized structural model used for computing $T_{\theta u}$ is the one accounting for the II order effects. Two alternative mass ratios are considered, namely μ=5% and μ=10%. For each mass ratio, the optimum frequency and damping ratios, r and ζ_t, are numerically found which minimize the filtered $T_{\theta u}$. The results of this design procedure are summarized in Table 4. Looking, for example, at the 10% mass ratio option, the optimal TMD turns out to be a SDOF appendage having mass m_t=9.00×10^5 kg, circular frequency ω_t=2.11 rad/s and damping ratio ζ_t=26.7%, or equivalently stiffness k_t=4.01 kN/mm and damping coefficient c_t=1.01 kNs/mm. As qualitatively indicated in Fig. 1, the SDOF appendage might be conceived, for instance, as a wide reinforced concrete platform resting on a system of appropriate bearings vertically aligned with the building internal columns, so as to distribute, as uniformly as possible, the additional weight of the device on the inner frames only, with the seismically-resisting perimeter MRFs remaining basically unaffected by TMD installation.

3.2 The seismic loading

The cost assessment procedure requires the evaluation of the structural response at M multiple hazard levels of increasing intensity, aimed at the definition of an equal number of $\phi^j_e - \theta_j$ pairs for every building storey. From these pairs, the curve analytically described by Eq. (7) is then derived for each storey, the function f being evaluated according to Eq. (10). In this work M=7 hazard levels are considered, whose probabilities of exceedance $P^j_{e/\tau}$ in the period τ and mean frequencies of exceedance ϕ^j_e are chosen as summarized in Table 5. Each level is described by a set of 20 time histories: 10 ground motions with 2 orthogonal components each. All sets are defined in accordance to the seismic hazard at the building site.

In particular, sets 5 to 7 are taken from the SAC steel research project (Somerville *et al.* 1997), and consist of recorded and simulated ground motions representing return periods of, respectively, 72 years (50% probability of exceedance in 50 years), 475 years (10% probability of exceedance in 50 years) and 2475 years (2% probability of exceedance in 50 years). All ground motions are rotated to 45° with respect to the fault in order to minimize directivity effects and are scaled such that, on average, their spectral ordinates match with a least square error fit the United States Geological Survey's (USGS) mapped spectral values at 0.3, 1.0 and 2.0 seconds, and an additional predicted value at 4.0 seconds. The weights ascribed to the four period points are 0.1 at the 0.3

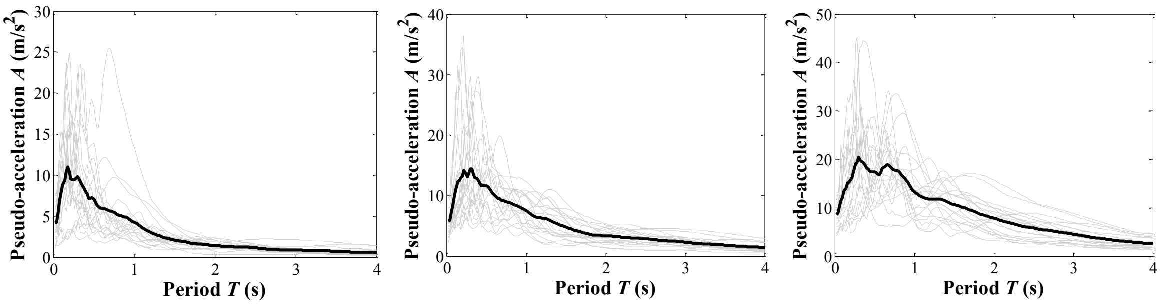

(a) Set # 5 (50/50) (b) Set # 6 (10/50) (c) Set # 7 (2/50)

Fig. 3 Pseudo-acceleration elastic spectra for ζ_s=5%. Thin grey lines: individual spectra; thick black line: mean spectra

second period point and 0.3 for the other three period points. The target spectra provided by USGS are for the SB/SC soil type boundaries, modified to be representative of soil type SD (stiff soil). Details can be found, for example, in Gupta and Krawinkler (1999).

Sets 1 to 4 are instead merely obtained through scaling set 5. The same scaling factor is used for all the records of each set and it is computed as the weighed sum of the ratios obtained dividing the corresponding USGS spectral values at 0.3, 1.0, 2.0 and 4.0 seconds by those corresponding to set 5, the weights being the same as described above.

In Fig. 3 the individual and mean 5% damped elastic pseudo-acceleration spectra are plotted for sets 5 to 7.

3.3 TMD performance in a traditional perspective

In order to traditionally evaluate TMD seismic performance under the seven sets of seismic records, twelve performance indices are here computed for each ground motion set. These indices are formulated as in the benchmark study by Ohtori *et al.* (2001), except that the mean response is here taken instead of the maximum response within each earthquake set.

The performance indices are dimensionless quantities defined by dividing the controlled by the uncontrolled response, falling into two main categories: building response and building damage. The first category comprises four peak response measures, namely: the maximum peak inter-storey drift ratio (J_1), the average peak inter-storey drift ratio (J_2), the maximum peak acceleration (J_3) and the peak base shear force (J_4), together with three root mean square (RMS) response measures, namely the maximum RMS inter-storey drift ratio (J_5), the maximum RMS acceleration (J_6) and the RMS base shear force (J_7). The second category comprises five damage measures, namely the maximum peak ductility factor at members' ends (J_8), the maximum dissipated energy factor at members' ends (J_9), the number of damaged members' ends (J_{10}), the maximum RMS ductility factor at members' ends (J_{11}) and the total dissipated energy factor (J_{12}), where the ductility factor denotes the instantaneous curvature divided by the yield curvature, the dissipated energy factor denotes the energy dissipated during the earthquake divided by the product of the yield curvature by the yield moment, and the damaged members' ends are meant as those in which the yield curvature is exceeded at least once during the earthquake. J_9, J_{10} and J_{12} have obviously only meaning for structures undergoing plastic deformations and are, therefore, undefined when the uncontrolled building remains elastic.

Table 6 TMD with μ=5%-Performance indices for the M=7 hazard levels

Set # j	J_1	J_2	J_3	J_4	J_5	J_6	J_7	J_8	J_9	J_{10}	J_{11}	J_{12}
1	0.84	0.80	0.92	0.72	0.58	0.69	0.50	0.82	n.a.	n.a.	0.54	n.a.
2	0.84	0.80	0.92	0.72	0.58	0.69	0.50	0.82	n.a.	n.a.	0.54	n.a.
3	0.84	0.80	0.92	0.72	0.58	0.69	0.50	0.81	0.02	0.13	0.53	0.01
4	0.84	0.81	0.93	0.74	0.69	0.70	0.50	0.77	0.68	0.38	0.69	0.72
5	0.85	0.83	0.94	0.81	0.72	0.74	0.55	0.78	0.51	0.49	0.71	0.54
6	0.91	0.91	1.02	0.99	0.91	0.81	0.68	0.88	0.73	0.96	0.98	0.62
7	0.92	0.95	1.03	0.98	0.99	0.90	0.82	0.91	0.81	0.98	1.03	0.84

Table 7 TMD with μ=10%-Performance indices for the M=7 hazard levels

Set # j	J_1	J_2	J_3	J_4	J_5	J_6	J_7	J_8	J_9	J_{10}	J_{11}	J_{12}
1	0.78	0.73	0.85	0.65	0.51	0.59	0.43	0.75	n.a.	n.a.	0.46	n.a.
2	0.78	0.73	0.85	0.65	0.51	0.59	0.43	0.75	n.a.	n.a.	0.46	n.a.
3	0.78	0.73	0.85	0.65	0.51	0.59	0.43	0.75	0.00	0.00	0.46	0.00
4	0.77	0.74	0.86	0.67	0.59	0.60	0.44	0.71	0.59	0.33	0.59	0.61
5	0.80	0.76	0.88	0.75	0.66	0.64	0.48	0.70	0.41	0.38	0.61	0.45
6	0.85	0.87	1.02	1.02	0.80	0.74	0.64	0.82	0.61	0.95	0.85	0.49
7	0.88	0.93	1.02	1.00	1.02	0.85	0.80	0.87	0.76	0.96	1.07	0.79

The computed indices are reported in Tables 6 and 7 for each earthquake set, respectively for μ=5% and μ=10%. Results are in line with expectations. The control performance improves as the mass ratio increases and as the hazard level diminishes; at the highest hazards, because of structural nonlinearity and TMD mistuning, the control action may even result detrimental in the light of some criteria (e.g., J_3>1 under sets 6 and 7). RMS response mitigation always exceeds peak response mitigation (except for J_5 under set 7, due to the RMS drift ratio being governed by permanent residual drifts), thus confirming TMDs' well-known property of more effectively reducing the post-peak response than the peak response to impulsive loads. Damage-related, energy-based indices are the criteria which highlight the most TMD merits, *per se* suggesting a satisfactory performance, particularly in global terms (J_{12}), even at high hazard levels.

The most remarkable result from Tables 6 and 7 is, however, the large variability in the values of the performance indices, depending on the adopted evaluation criterion and on the considered hazard level. Even apparently similar indices, such as J_1 and J_2 (both related to peak drift ratios, although respectively in maximum and average terms), show a different dependence on the hazard level, much stronger for J_2 then for J_1. Such variability highlights the need to find a unifying, concise cost-related performance measure capable to replace the numerous individual indices and to appropriately weigh the different economic significance of the various hazard scenarios. In the next Subsection, lifetime cost will be proposed as this unifying performance measure, and the peak drift ratio is the EDP on whose basis that cost will be computed. With this in mind, another remarkable result from Tables 6 and 7 is that TMD's effects on the peak drift ratio (described by J_1 and J_2) appear limited and heavily degraded as the seismic hazard increases. For example, as the hazard increases from 1 to 7, the average peak drift ratio (J_2) varies from 0.80 to 0.95 for μ=5%

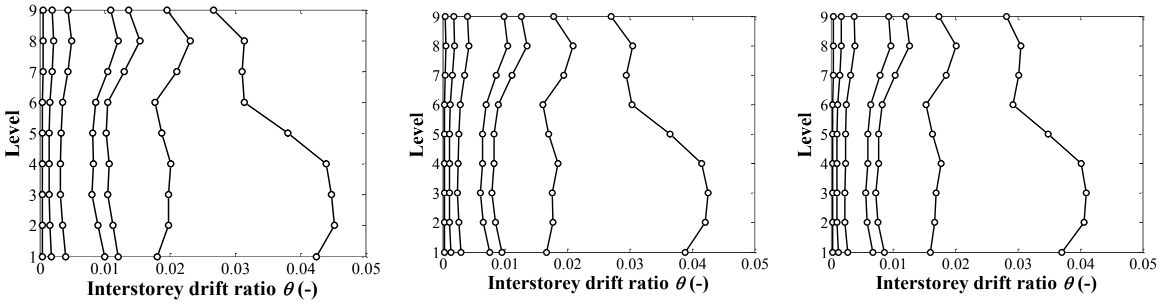

(a) μ=0% (uncontrolled) (b) μ=5% (controlled) (c) μ=10% (controlled)

Fig. 4 Inter-storey drift ratios along the height of the building for the three control cases. The 7 curves in each graph correspond to the 7 hazard levels (orderly rightwards)

and from 0.73 to 0.93 for μ=10%. In more details, this also appears in Fig. 4, where the peak drift ratios are plotted along the height of the building for each hazard level. In agreement with Gupta and Krawinkler (1999), drift ratio demands of about 1%, 2% and 4% in average are observed at, respectively, the 50/50, the 10/50 and the 2/50 hazard levels. No large differences between the uncontrolled and the controlled curve are noticeable, particularly at the highest hazard levels. Such discouraging results help to explain why TMD are commonly believed to be of scarce practical interest in controlling the seismic response of structures in the nonlinear range. The next Subsection will reconsider this point in the light of a life-cycle cost approach.

3.4 TMD performance in a life-cycle cost perspective

The procedure presented in Section 2.3 is applied to the 9-storey SAC building, with and without control. For each storey level, the θ_j term of each $\phi_e^j - \theta_j$ pair is computed from nonlinear analyses as the set-EDP. The function $f(\theta)$ defined by Eq. (10) is derived through a numerical minimization, the optimal weight turning out to be γ=0.8.

The procedure is detailed in Fig. 5 for the 8-th storey level, the one contributing the most to the total building cost, and for the three control cases, i.e., μ=0% (uncontrolled), μ=5% and μ=10%. The black markers represent the "forward step" of the procedure (time-history analysis), the white markers the "backward step" (extraction of the exceedance and occurrence frequencies for each damage state). Similar curves are obtained for the other storeys, as well as for the maximum drift ratio among all the storeys.

Once the occurrence frequency is evaluated for all storey levels and for all damage states, the lifetime costs can be computed using Eq. (5) and Tables 1 to 3 and assuming, for the present example, a lifetime period t=50 years and a momentary discount rate λ=4%/year.

Results are reported in Figs. 6 and 7. In Fig. 6 the lifetime cost is decomposed, for the uncontrolled and controlled cases, into the seven damage states for each storey level. Since the cost related to the first damage state ("1-None") is null, only six damage states are actually represented in the bar graph using rectangles of different colours, from the second one (on the left) to the seventh one (on the right). For the two controlled cases, a white rectangle is added on the right, for comparison's sake, to represent the complement to the uncontrolled cost. It clearly results that most damage cost is inflicted within the forth damage state ("4-Moderate") and secondarily within the fifth one ("5-Heavy"), which achieve the most expensive combination of occurrence

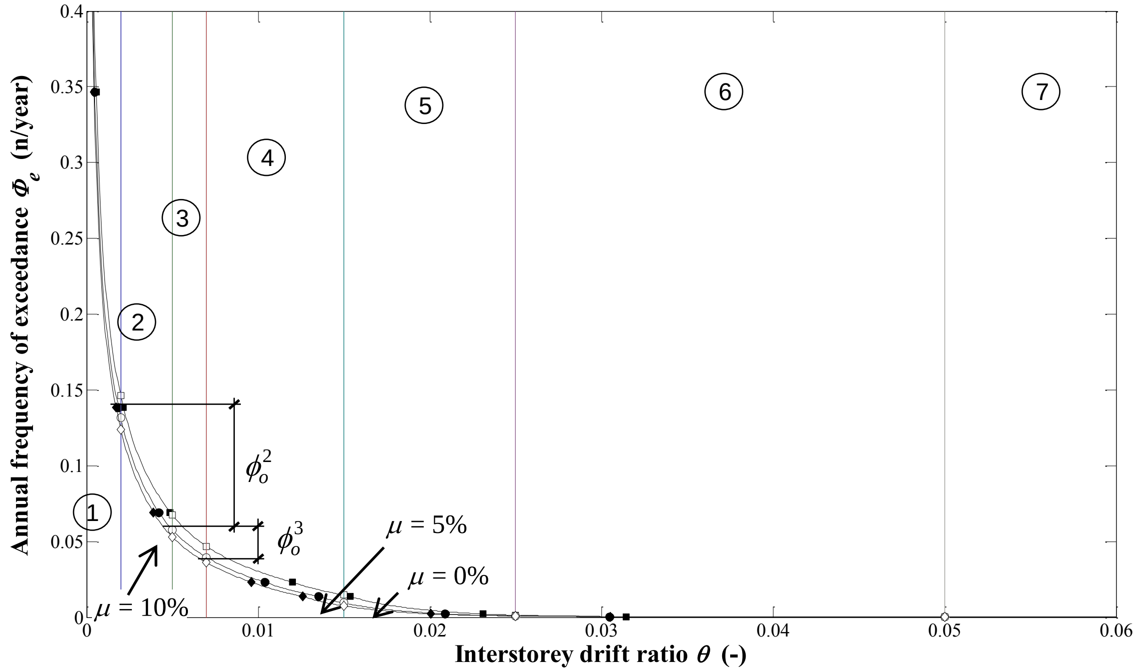

Fig. 5 Annual frequency of exceedance as a function of the inter-storey drift ratio, for the 8-th storey level and respectively: μ=0% (square markers); μ=5% (circles); μ=10% (triangles). Black markers: from analyses; white markers: from fitting

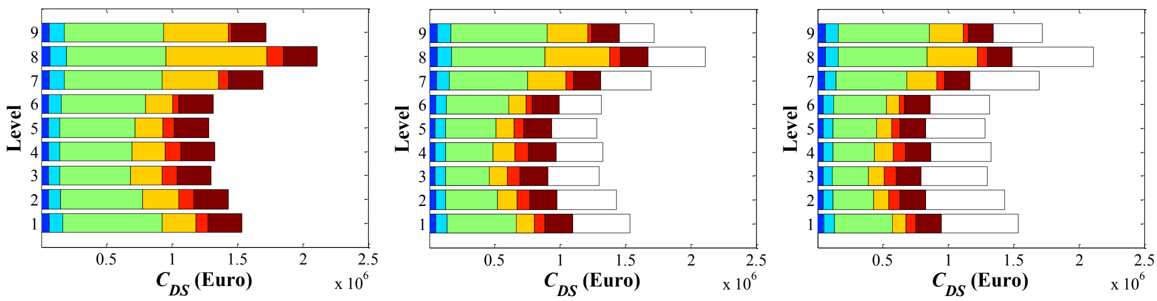

(a) μ=0% (uncontrolled) (b) μ=5% (controlled) (c) μ=10% (controlled)

Fig. 6 Lifetime costs for the uncontrolled and controlled cases, decomposed among storey levels and damage states. Legend for the damage states, from left to right: 1 (dark blue, not shown); 2 (blue); 3 (azure); 4 (green); 5 (orange); 6 (red); 7 (brown)

probability and damage severity, thus contributing the most to the overall lifetime cost. These intermediate damage states are those where TMD cost-effectiveness achieves its best. Within the forth damage state, the TMD reduces the building cost to 76% of its uncontrolled value for μ=5%, and to 67% for μ=10%; within the fifth damage state, the reduction is even larger, to respectively 62% for μ=5% and 50% for μ=10%. The third most expensive damage state is the seventh one, corresponding to collapse ("7-Destroyed"). Note that the collapse cost is the same at every storey level, because of the assumption that the collapse of any one storey implies the collapse of the

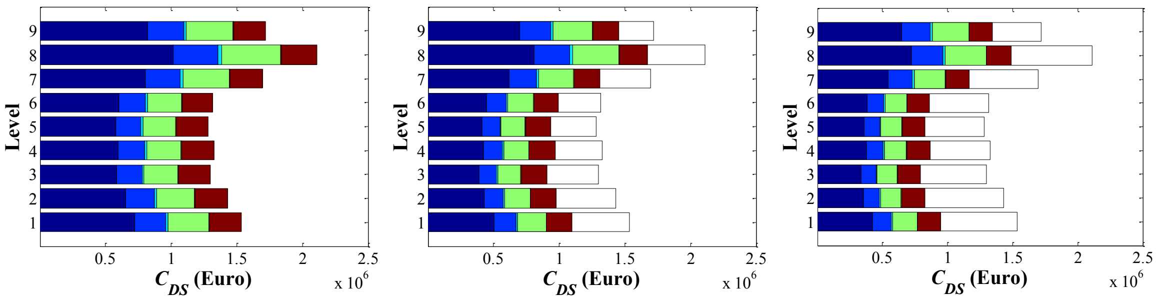

(a) μ=0% (uncontrolled) (b) μ=5% (controlled) (c) μ=10% (controlled)

Fig. 7 Lifetime costs for the uncontrolled and controlled cases, decomposed among storey levels and cost categories. Legend for the cost categories, from left to right: C^i_{dam} (dark blue); C^i_{con} (blue); C^i_{ren} (azure); C^i_{inc} (green); $C^i_{inj,m}$ (orange); C^i_{inj} (red); C^i_{fat} (brown)

entire building. Even if the cost reduction within the collapse damage state is considerably less than for the intermediate damage states, it still keeps to an acceptable 81% for μ=5% and 73% for μ=10%.

Fig. 7 is the analogue of Fig. 6, except that the cost is now decomposed in cost categories instead of damage states. For any of the three control cases, the category which contributes the most is damage repair (about 47%), followed by income (about 20%), fatalities (about 16%) and loss of content (about 15%). The other three categories, i.e., rental, minor and serious injuries, contribute for about 1% each.

Summing along the building height, the total damage cost (C_{DS}) for the uncontrolled structure turns out to be $13.7 \cdot 10^6$ Euro. For the 5% and 10% controlled cases, it drops to, respectively, $10.3 \cdot 10^6$ Euro and $9.1 \cdot 10^6$ Euro, i.e., to 75% and 66% of the uncontrolled cost. Smeared on the total area of the nine above-ground floors, these total costs are equivalent to unit damage costs of, respectively, 729 Euro/m^2, 548 Euro/m^2 and 485 Euro/m^2. The lifetime cost saved by the TMD is therefore $3.4 \cdot 10^6$ Euro for μ=5% and $4.6 \cdot 10^6$ Euro for μ=10%; although a detailed cost-benefit analysis exceeds the scope of this paper, preliminary estimates indicate that these cost savings are much larger than the cost necessary for designing, building and maintaining the TMD system.

The whole LCC assessment procedure was finally repeated using a mechanically linear model instead of the bilinear one. Only a slight improvement was observed in TMD cost-effectiveness with respect to the nonlinear case: for the 5% and 10% controlled cases, the total lifetime cost was found to be, respectively, 70% (instead of 75%) and 60% (instead of 66%) of the uncontrolled response. This result indicates that the influence of structural nonlinearity on TMD convenience may be not as dramatic as commonly expected.

4. Conclusions

In this paper a methodology for evaluating the cost-effectiveness of passive TMDs on nonlinear MRF building structures located in high seismicity regions is presented and exemplified on the 9-storey SAC steel benchmark building. The method is a slight variant of previous LCC multi-hazard approaches, relying on MSDA to compute the occurrence probability of multiple damage states expressed in terms of peak inter-storey drift ratios. By estimating, for the original uncontrolled building as well as for two possible TMD installations (respectively μ=5% and 10%), the expected cost of future earthquake damages and losses, the illustrative case study infers the economic advantage of implementing the control action.

Results confirm that TMDs on nonlinear structures perform acceptably well under moderate earthquake loading, when the structure remains linear or weakly nonlinear, but may lose effectiveness (especially in peak response mitigation) under the most severe ground shaking, when strong nonlinearities occur. Traditional performance criteria, computed under increasing hazard levels, prove inadequate to univocally and concisely assess TMD adequacy, because: (i) different criteria give different indications; (ii) these criteria alone cannot weigh, on a physically sound, economically founded basis, the relative significance of the various hazard levels.

By determining, for each damage state, its probability of occurrence and its expected lifetime cost, the LCC approach herein proposed can provide, instead, a rational and comprehensive measure of TMD performance, directly expressed in monetary terms and thus immediately useable for decision making purposes. In the present case study, the 5% and 10% TMD options are shown to reduce the building lifetime cost to, respectively, 75% and 66%. Reductions are particularly conspicuous for costs related to those intermediate damage states (“4-Moderate” and “5-Heavy”) which, achieving the most expensive combination of occurrence probability and damage severity, contribute the most to the overall lifetime cost. Although a thorough estimation of costs associated to TMD design, building and maintenance is not in the scope of the present paper, preliminary estimations indicate that TMD costs are largely compensated by building LCC savings.

It can be concluded that, for typical middle-rise steel MRF office buildings located in high seismic areas, despite the poor control performance observed under the most severe earthquake records, the seismic cost-effectiveness of TMDs may be considerably larger than traditional performance criteria would suggest, only slightly inferior to that found in the assumption of a linear structural behaviour, and anyway of remarkable practical interest.

Extending the present analysis to further case studies, including TMD costs into the LCC evaluation and adopting the LCC as the objective function for TMD optimal design will be the scope of future work.

References

Beck, J.L., Porter, K.A. and Shaikhutdinov, R.V. (2003), “Simplified estimation of seismic life-cycle costs”, Eds., Frangopol, D.M., Bruhwiler, E., Faber, M.H. and Adey, B., *Life-cycle performance of deteriorating structures: assessment, design, and management*, 229-236.

Bernal, D. (1996), “Influence of ground motion characteristic on the effectiveness of tuned mass dampers”, *Proceedings 11th World Conference Earthquakes Engineering*, Acapulco.

Chowdhury, A.H., Iwuchukwu, M.D. and Garske, J.J. (1985), “Past and future of seismic effectiveness of tuned mass dampers”, *Proceedings 2nd Int. Symp. on Structural Control*, Ontario, Canada.

FEMA-273 (1997), *NEHRP guidelines for seismic rehabilitation of buildings*, Federal Emergency Management Agency, Washington, DC.

FEMA-350 (2000), *Recommended seismic design criteria for new steel moment-frame buildings*, Federal Emergency Management Agency, Washington, DC.

Fragiadakis, M. and Lagaros, N.D. (2011), “An overview to structural seismic design optimisation frameworks”, *Comput. Struct.*, **89**(11), 1155-1165.

Ghobarah, A., Abou-Elfath, H. and Biddah, A. (1999), “Response-based damage assessment of structures”, *Earthq. Eng. Struct. Dyn*., **28**(1), 79-104.

Ghobarah, A. (2004), "On drift limits associated with different damage levels", *Proceedings International Workshop Performance-Based Seismic Design - Concepts and Implementation*, Bled, Slovenia.
Goulet, C.A., Haselton, C.B., Mitrani-Reiser, J., Beck, J.L., Deierlein, G.G., Porter, K.A. and Stewart, J.P. (2007), "Evaluation of the seismic performance of a code-conforming reinforced-concrete frame building - from seismic hazard to collapse safety and economic losses", *Earthq. Eng. Struct. Dyn*., **36**(13), 1973-1997.
Gupta, A. and Krawinkler, H. (1999), *Seismic demands for performance evaluation of steel moment resisting frame structures*, The John A. BLume Earthquake Engineering Center, Stanford University, Stanford, CA.
Hahm, D., Ok, S.Y., Park, W., Koh, H.M. and Park, K.S. (2013), "Cost-effectiveness evaluation of an MR damper system based on a life-cycle cost concept", *KSCE J. Civil Eng.*, **17**(1), 145-154.
Hoang, N., Fujino, Y. and Warnitchai, P. (2008), "Optimal tuned mass damper for seismic applications and practical design formulas", *Eng. Struct*., **30**(3), 707-715.
Homma, S., Maeda, J. and Hanada, N. (2009), "The damping efficiency of vortex-induced vibration by tuned-mass damper of a tower-supported steel stack", *Wind Struct.*, **12**(4), 333-347.
Kappos, A.J. and Dimitrakopoulos, E.G. (2008), "Feasibility of pre-earthquake strengthening of buildings based on cost-benefit and life-cycle cost analysis, with the aid of fragility curves", *Nat. Hazard.*, **45**(1), 33-54.
Kaynia, A.M., Veneziano, D. and Biggs, J.M. (1981), "Seismic effectiveness of tuned mass dampers", *J. Struct. Eng.*, **107**(8), 1465-1484.
Kircher, C.A., Whitman, R.V. and Holmes, W.T. (2006), "Hazus earthquake loss estimation methods", *Nat. Hazard.*, **7**(2), 45-59.
Lagaros, N.D., Fotis, A.D. and Krikos, S.A. (2006), "Assessment of seismic design procedures based on the total cost", *Earthq. Eng. Struct. Dyn*., **35**(11), 1381-1401.
Lukkunaprasit, P. and Wanitkorkul, A. (2001), "Inelastic buildings with tuned mass dampers under moderate ground motions from distant earthquakes", *Earthq. Eng. Struct. Dyn*., **30**(4), 537-551.
Matta, E., De Stefano, A. and Spencer, B.F.Jr. (2009), "A new passive rolling-pendulum vibration absorber using a non-axial-symmetrical guide to achieve bidirectional tuning", *Earthq. Eng. Struct. Dyn*., **38**(15), 1729-1750.
Matta, E. (2011), "Performance of tuned mass dampers against near-field earthquakes", *Struct. Eng. Mech.*, **39**(5), 621-642.
Matta, E. (2013), "Effectiveness of tuned mass dampers against ground motion pulses", *J. Struct. Eng.*, **139**(2), 188-198.
Mitropoulou, C.C., Lagaros, N.D. and Papadrakakis, M. (2011), "Life-cycle cost assessment of optimally designed reinforced concrete buildings under seismic actions", *Reliab. Eng. Syst. Saf.*, **96**(10), 1311-1331.
Ohtori, Y., Christenson, R.E., Spencer, Jr., B.F. and Dyke, S.J. (2004), "Benchmark control problems for seismically excited nonlinear buildings", *J. Eng. Mech*., **130**(4), 366-385.
Pinkaew, T., Lukkunaprasit, P. and Chatupote, P. (2003), "Seismic effectiveness of tuned mass dampers for damage reduction of structures", *Eng. Struct*., **25**(1), 39-46.
Ruiz, S.E. and Esteva, L. (1997), "About the effectiveness of tuned mass dampers on nonlinear systems subjected to earthquakes", Eds., Manolis, G.D., Beskos, D.E. and Brebbia, C.A., *Earthquake Resistant Engineering Structures*, *Adv. Earthq. Eng.*, **2**, 311-320.
Sadek, F., Mohraz, B., Taylor, A.W. and Chung, R.M. (1997), "A method of estimating the parameters of tuned mass dampers for seismic applications", *Earthq. Eng. Struct. Dyn*., **26**(6), 617-635.
Sanchez-Silva, M. and Rackwitz, R. (2004), "Socioeconomic implications of life quality index in design of optimum structures to withstand earthquakes", *J. Struct. Eng*., **130**(6), 969-977.
Sladek, J.R. and Klingner, R.E. (1983), "Effect of tuned mass dampers on seismic response", *J. Struct. Eng*., **109**(8), 2004-2009.
Somerville, P., Smith, N., Punyamurthula, S. and Sun, J. (1997), *Development of ground motion time histories for phase 2 of the FEMA/SAC steel project*, SAC Background Document, Report No. SAC/BD-97/04.
Soong, T.T. and Dargush, G.F. (1997), *Passive energy dissipation systems in structural engineering*, John

Wiley & Sons, New York, USA.
Soto-Brito, R. and Ruiz, S.E. (1999), "Influence of ground motion intensity on the effectiveness of tuned mass dampers", *Earthq. Eng. Struct. Dyn*., **28**(11), 1255-1271.
Taflanidis, A.A. and Beck, J.L. (2009), "Life-cycle cost optimal design of passive dissipative devices", *Struct. Saf.*, **31**(6), 508-522.
Vamvatsikos, D. and Cornell, C.A. (2002), "Incremental dynamic analysis", *Earthq. Eng. Struct. Dyn*., **31**(3), 491-514.
Villaverde, R. and Koyama, L.A. (1993), "Damped resonant appendages to increase inherent damping in buildings", *Earthq. Eng. Struct. Dyn*., **22**(6), 491-507.
Warburton, G.B. (1982), "Optimum absorber parameters for various combinations of response and excitation parameters", *Earthq. Eng. Struct. Dyn*., **10**(3), 381-401.
Wen, Y.K. and Kang, Y.J. (2001), "Minimum building life-cycle cost design criteria. II: Applications", *J. Struct. Eng*., **127**(3), 338-346.
Wong, K.K.F. (2008), "Seismic energy dissipation of inelastic structures with tuned mass dampers", *J. Eng. Mech*., **134**(2), 163-172.
Wong, K.K.F. and Harris, J.L. (2012), "Seismic damage and fragility analysis of structures with tuned mass dampers based on plastic energy", *Struct. Des. Tall Spec. Build*., **21**(4), 296-310.
Zhang, Z. and Balendra, T. (2013), "Passive control of bilinear hysteretic structures by tuned mass damper for narrow band seismic motions", *Eng. Struct.*, **54**, 103-111.

CC